6 Sequence-specific knockdown of EWS-FLI1 by targeted, non-viral delivery of siRNA inhibits tumor growth in a murine model of metastatic Ewing's sarcoma[†]

6.1 Abstract

Systemic delivery of nucleic acid molecules is one of the major hurdles limiting the application of siRNA-based therapeutics for cancer treatment. Multifunctional nanoparticles are being investigated as systemic, nonviral nucleic acid delivery systems, and here we describe the use of cyclodextrin-containing polycations (CDP) to interact with small interfering RNA (siRNA) molecules to form nanoparticles that can be modified with transferrin (Tf) for targeting to transferrin receptor (TfR)-overexpressing tumor cells. Twice-weekly intravenous injections of Tf-targeted nanoparticles formed with an siRNA targeting the EWS-FLI1 oncogenic fusion protein are able to achieve sequence-specific knockdown of the EWS-FLI1 gene in vivo, leading to tumor growth inhibition in a disseminated model of Ewing's sarcoma. Removal of the targeting ligand or the use of a control siRNA sequence eliminates the anti-tumor effects. Additionally, no abnormalities in interleukin-12 and interferon-alpha, liver and kidney function tests, complete blood counts, or pathology of major organs are observed after injection of the nanoparticles. These data provide strong evidence for the safety and efficacy of this targeted, non-viral siRNA delivery system.

[†] Adapted from: Hu-Lieskovan, S., Heidel, J.D., Bartlett, D.W., Davis, M.E. and Triche, T.J. (2005) Sequence-specific knockdown of EWS-FLI1 by targeted, nonviral delivery of small interfering RNA inhibits tumor growth in a murine model of Ewing's sarcoma. *Cancer Res*, **65,** 8984-8992.

6.2 Introduction

Ewing's family of tumors (EFT) is a poorly differentiated mesenchymal malignancy that arises in bone or soft tissue. It is the second most common primary osseous malignancy in childhood and adolescence (1). Historical data show that virtually all patients die from metastases (e.g., <5% survival after localized therapy (2)). Systemic chemotherapy has improved survival of patients with localized disease, but patients with metastatic disease rarely benefit from continued therapy (3). A major factor contributing to this outcome is the development of multi-drug resistance by the time patients are treated for metastasis. The translocation t(11;22) is commonly detected in EFT and produces the chimeric EWS-FLI1 fusion gene found in 85% of EFT patients (3). The EWS domain replaces the normal transcriptional activator domain in the 5' region of the FLI1 DNA-binding protein, leading to altered transcriptional activation that contributes to the tumorigenic phenotype (1). Reduction of the EWS-FLI1 protein in EFT cells in vitro or in subcutaneous xenograft tumors by antisense oligonucleotides complementary to EWS-FLI1 mRNA results in decreased proliferation (4-6), suggesting a potential therapeutic intervention directed at this tumor-specific chimeric gene. Small interfering RNAs (siRNAs) have recently been shown to silence the EWS-FLI1 gene and suppress proliferation of an EFT cell line in vitro (7-9). To build upon these previous studies, the current study explores the use of systemically delivered siRNA against EWS-FLI1 to inhibit growth and dissemination of EFT cells in a xenograft model of Ewing's sarcoma.

As discussed in Chapter 4, nanoparticle carriers offer several features that make them attractive for systemic siRNA delivery. Cyclodextrin-containing polycations (CDP) can interact with small interfering RNA (siRNA) molecules to form nanoparticles that are

approximately 60-80 nm in diameter. The modular design of these nanoparticles enables modification with PEG molecules for steric stabilization and Tf targeting ligands for uptake by TfR-overexpressing tumor cells. The nanoparticles protect the nucleic acid payload from nuclease degradation, do not aggregate at physiological salt concentrations, and cause minimal erythrocyte aggregation and complement fixation. Here, we investigate their ability to deliver a therapeutic siRNA to tumor cells in vivo after intravenous administration.

The EFT cell line, TC71, is used to create a disseminated model of Ewing's sarcoma in NOD/scid mice. The TC71 cells engineered to express the luciferase gene (TC71-Luc) are injected by low-pressure tail-vein injection to mimic the metastatic process. The most common engraftment sites are lung, vertebral column, pelvis, femur, and soft tissue, corresponding to the most frequently observed sites for metastases in EFT patients (10). Live-animal bioluminescent imaging (BLI) is used to noninvasively track the growth of metastases in mice. We test the ability of targeted, non-viral delivery of siRNA against EWS-FLI1 to safely limit bulk metastatic tumor growth and prevent establishment of bulk metastatic disease from microscopic metastatic disease. We prove here the hypothesis that the targeted, non-viral delivery of siRNA can safely abrogate EWS-FLI1 expression and inhibit metastatic Ewing's tumor growth in vivo.

6.3 Materials and methods

6.3.1 siRNA sequences

siRNA targeting luciferase (siGL3), the breakpoint of EWS-FLI1 (siEFBP2), a mutated negative control for siEFBP2 (siEFBP2mut), and a non-targeting control sequence (siCON1) were obtained from Dharmacon Research, Inc..

siGL3:
5'-----CUUACGCUGAGUACUUCGAdTdT
dTdTGAAUGCGACUCAUGAAGCU-----5'

siEFBP2(7):
5'---GCAGAACCCUUCUUAUGACUU
UUCGUCUUGGGAAGAAUACUG---5'

siEFBP2mut(7):
5'---GCAGAACCAGUCUUAUGACUU
UUCGUCUUGGUCAGAAUACUG---5'

siCON1:
5'---UAGCGACUAAACACAUCAAUU
UUAUCGCUGAUUUGUGUAGUU---5'

6.3.2 In vitro down-regulation of EWS-FLI1 in an EFT cell line

TC71 cells were grown on 6-well plates in RPMI 1640 with 10% FBS (no antibiotics) until they reached 30% confluency. siRNA was complexed with Oligofectamine (Invitrogen) according to the manufacturer's instructions. The resulting formulations were applied to each well at a final concentration of 100 nM. All transfected cells were harvested at 48 h and gene expression was assessed by Western blot analysis. Primary monoclonal antibodies against the C-terminal region of FLI1 were obtained from BD Biosciences. Polyclonal antibodies against β-Actin were obtained from Santa Cruz Biotechnology.

6.3.3 Injection of mice with TC71-Luc cells

TC71-Luc cells were grown in RPMI 1640 supplemented with 10% FBS and antibiotics (penicillin/streptomycin) and subsequently trypsinized and resuspended in serum-free RPMI 1640 for injection. Each mouse was injected with $5x10^6$ TC71-Luc cells by tail vein injection of 0.2 mL of the cell suspension. Mice were treated according to the NIH Guidelines for Animal Care and as approved by the Caltech Institutional Animal Care and Use Committee. All mice were 6-8 weeks of age at the time of injection.

6.3.4 Bioluminescent imaging of the mice

Longitudinal imaging of the mice was performed using the Xenogen IVIS 100 imaging system. D-luciferin (Xenogen) was dissolved in PBS at 15 g L^{-1}, and 0.2 mL of the 15 g L^{-1} luciferin solution was injected i.p. 10 minutes before measuring the light emission. Mice were anesthetized with an initial dose of 5% isoflurane followed by a maintenance dose of 2.5% isoflurane. Bioluminescent signals were quantified using Living Image software (Xenogen).

6.3.5 Formulation of non-viral, siRNA-containing nanoparticles for in vivo administration

Before addition to the nucleic acid, the CDP was mixed with AD-PEG at a 1:1 AD-PEG:β-CD (mol:mol) ratio in water. Targeted nanoparticles also contained transferrin-modified AD-PEG (AD-PEG-Tf) at a 1:1000 AD-PEG-Tf:AD-PEG (w:w) ratio. The mixture of CDP, AD-PEG, and AD-PEG-Tf in water was then added to an equal volume of siRNA in water such that the ratio of positive charges from CDP to negative charges from the nucleic acid was equal to the desired charge ratio of 3 (+/-).

An equal volume of 10% (w/v) glucose in water was added to the resulting nanoparticles to give a final concentration of 5% (w/v) glucose suitable for injection.

6.3.6 Consecutive-day delivery of siRNA to tumors in vivo

Mice with successful tumor cell engraftment received injection of formulations containing siRNA against luciferase (siGL3), EWS-FLI1 (siEFBP2) or a control sequence (siCON1) on two or three consecutive days as indicated. Each mouse (~20 g) received 0.2 mL of the appropriate formulation, containing 50 μg of siRNA corresponding to a 2.5 mg/kg dose, by low-pressure tail-vein injection using a 1-mL syringe and a 27-gauge needle.

6.3.7 Real Time Quantitative RT-PCR (Q-RT-PCR)

Total cellular RNA was isolated using RNA STAT-60 (Tel-Test) from homogenized tumors. cDNA was synthesized from 2 μg of DNase I (Invitrogen)-treated total RNA in a 42μl reaction volume using oligo–dT and Superscript II (Invitrogen) for 60 min at 42°C following suppliers' instructions. PCR primers were designed with MacVector 7.0 (Accelrys). The sequences are:

EWS-FLI1, forward, 5'-CGACTAGTTATGATCAGAGCAGT-3',

reverse, 5'-CCGTTGCTCTGTATTCTTACTGA-3';

β-Actin, forward, 5'-GCACCCCGTGCT GCTGAC-3',

reverse, 5'-CAGTGGTACGGCCAGAGG-3'.

PCR was performed as described previously (11). PCR conditions were 95°C for 900 s; 40 cycles of 95°C for 15 s, 60°C for 30 s, 72°C for 30 s; and a final denaturing stage from 60°C to 95°C. All PCR products were analyzed on a 1% agarose gel and a single band was observed except for negative controls. The reproducibility was evaluated by at least

three PCR measurements. The expression level of the target gene was normalized to internal β-actin and the mean and standard deviation of the target/β-actin ratios were calculated for sample-to-sample comparison.

6.3.8 Long-term delivery of siRNA to tumors in vivo

Fifty female NOD/scid mice were injected with $5x10^6$ TC71-Luc cells as described above. Immediately after cell injection, each mouse received an additional injection of 0.2 mL of one of the following formulations (n = 10 mice per group): 5% glucose (group A); naked siEFBP2 (group B); targeted nanoparticles containing siCON1 (group C); targeted nanoparticles containing siEFBP2 (group D); or non-targeted nanoparticles containing siEFBP2 (group E). Formulations were administered twice-weekly for four weeks. Images were taken immediately after the first injections for quality control of the injections and twice-weekly immediately before the injection of the formulations. We continued to monitor the tumor signal in the mice receiving targeted (group D) and non-targeted (group E) siEFBP2 formulations for an additional three weeks or until tumor burden required euthanization of the mice.

6.3.9 Toxicity, immune response, and pathology studies

Female C57BL/6 mice (Jackson Laboratories) were 6-8 weeks of age at the time of injection. To measure plasma cytokine levels, blood was harvested from mice 2 h and 24 h post-injection by cardiac puncture and plasma was isolated using Microtainer tubes (Becton Dickinson). Whole blood was used for complete blood count (CBC) analyses, and plasma was used for all liver enzyme and cytokine analyses. IL-12 (p40) (BD Biosciences) and IFN-α levels (PBL Biomedical Laboratories) were measured by ELISA according to the manufacturer's instructions. Major organs of the NOD/scid mice after

long-term treatment studies were collected, formalin-fixed and processed for routine hematoxylin and eosin staining using standard methods. Images were collected using a Nikon epifluorescent microscope with a DP11 digital camera.

6.4 Results

6.4.1 siRNA mediates down-regulation of EWS-FLI1 in cultured TC71 cells

Using a previously reported siRNA sequence targeting the EWS-FLI1 breakpoint (siEFBP2)(7), we observed comparable and significant (greater than 50%) reduction in EWS-FLI1 protein levels after Oligofectamine-mediated transfection (Figure 6.1). Delivery of a mutant siRNA sequence (siEFBP2mut) failed to elicit such down-regulation.

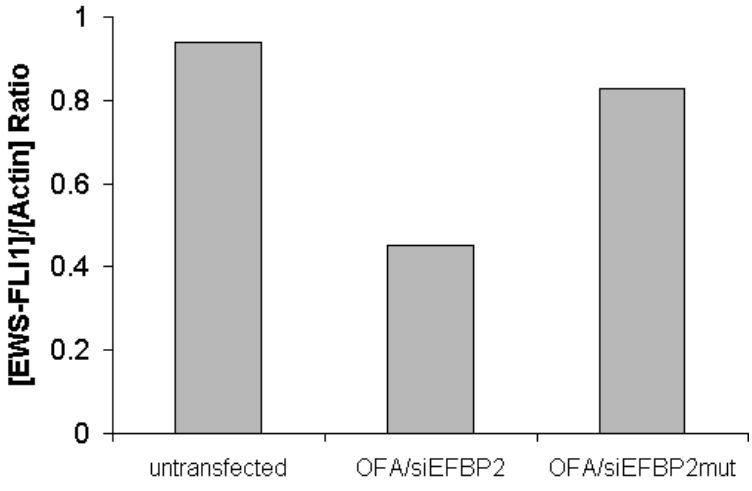

Figure 6.1. In vitro knockdown of EWS-FLI1 in cultured TC71 cells. At 48 h post-transfection, cells were lysed and total cell protein was denatured, electrophoresed, and transferred to a PVDF membrane that was probed with antibodies to EWS-FLI1 or actin (siEFBP2mut: mutant negative control). Average band intensities were determined by densitometry and the ratio of EWS-FLI1 to actin intensities was calculated.

6.4.2 Formulated siRNA against EWS-FLI1 inhibits tumor growth in vivo

Mice with successful engraftment of TC71-Luc cells were randomly selected for treatment with targeted nanoparticles containing siEFBP2 on two consecutive days.

Assessment of the EWS-FLI1 expression in the tumors treated with two consecutive siEFBP2 formulations showed a 60% down-regulation of EWS-FLI1 RNA level compared to siCON1-treated tumors (p=0.046). (Figure 6.2). Therefore, the delivery of targeted nanoparticles containing siEFBP2 is able to reduce EWS-FLI1 expression in the established tumors.

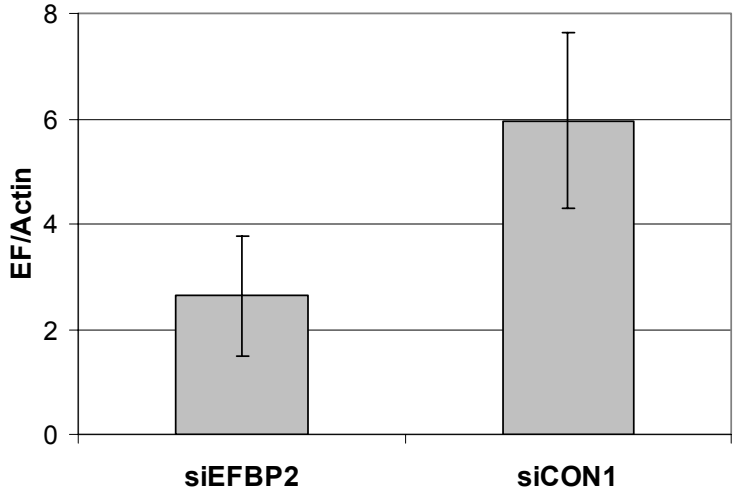

Figure 6.2. In vivo knockdown of EWS-FLI1 RNA levels in metastasized TC71-Luc tumors in mice. Tf-targeted nanoparticles containing 2.5 mg/kg of siEFBP2 or siCON1 were administered intravenously on days 19 and 20 after injection of TC71-Luc cells. Tumors were harvested on the third day. RNA was extracted and EWS-FLI1 level was determined by Q-RT-PCR.

6.4.3 Long-term, twice-weekly administration of targeted, formulated siEFBP2 inhibits tumor cell engraftment

To investigate the potential for tumor growth inhibition as a result of EWS-FLI1 knockdown, we employed a long-term treatment regimen in which formulations were administered twice weekly beginning the same day as injection of TC71-Luc cells. These studies allowed for the more careful investigation of the effects of variations in the formulation conditions. Targeted nanoparticles containing siEFBP2 (group D) dramatically inhibited the engraftment of TC71-Luc cells, with only 20% of the mice

showing any tumor growth compared to 90-100% in other treatment groups (Figure 6.3). Neither the mice receiving naked siEFBP2 (group B) nor those receiving targeted delivery of siCON1 (group C) showed any difference in tumor engraftment compared to the control group that received only the 5% glucose carrier solution (group A). Interestingly, tumors in mice treated with non-targeted nanoparticles containing siEFBP2 showed a delayed progression of tumor engraftment compared to the control groups. Once significant tumors were established, however, the tumors seemed to grow at a rate unaffected by continued treatment with the non-targeted nanoparticles containing siEFBP2 (Figure 6.4). The tumor signal was monitored in the mice receiving targeted (group D) and non-targeted (group E) nanoparticles containing siEFBP2 for an additional three weeks until the tumor burden required euthanization of the mice. Whereas most of the mice receiving non-targeted nanoparticles developed very large tumors, the majority of the mice receiving targeted nanoparticles showed little or no tumor signal (Figure 6.3). We conclude that treatment with the targeted nanoparticles containing siEFBP2 prevented the tumor cell engraftment in these mice and slowed the growth of any tumors that did develop.

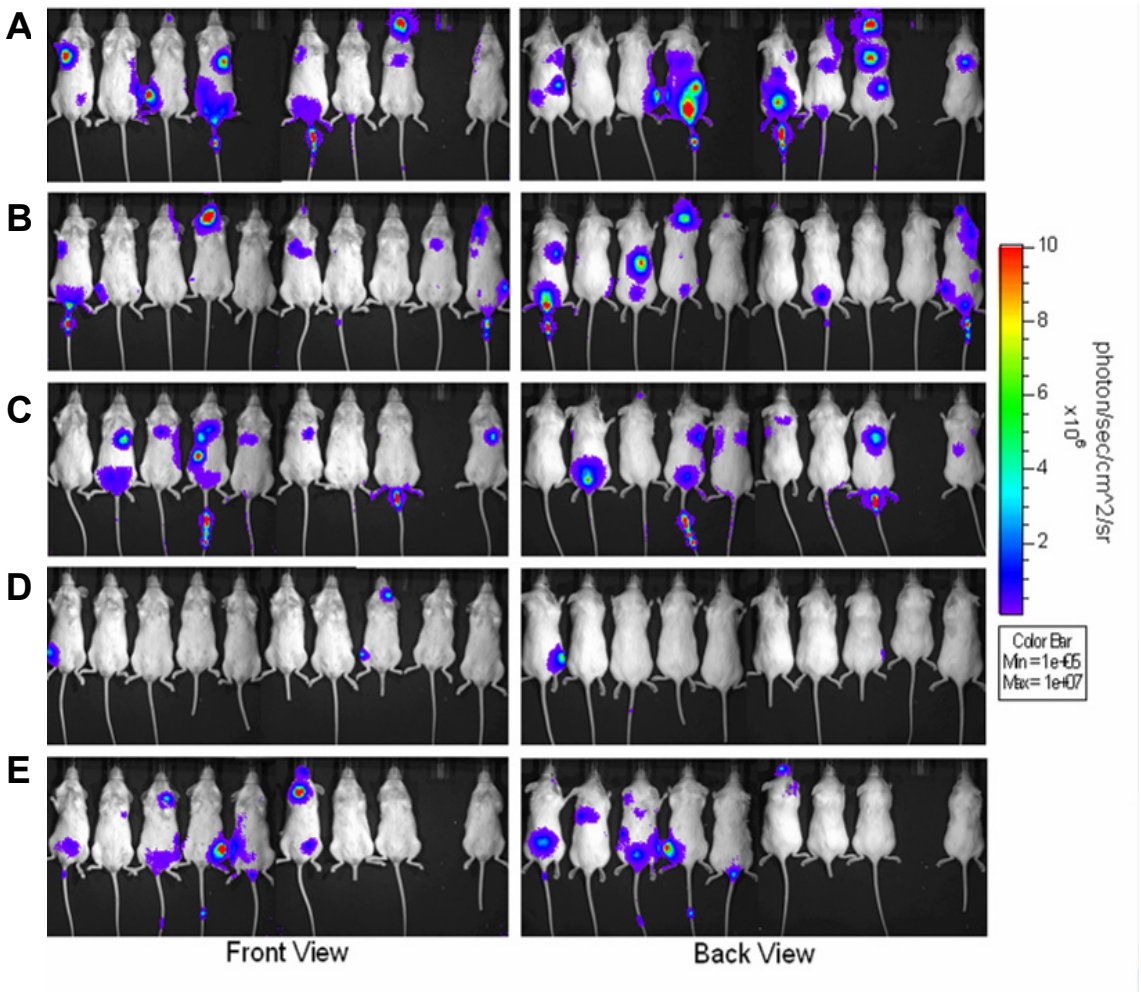

Figure 6.3. Bioluminescent images of the remaining mice from all treatment groups in NOD/scid mice 3.5 weeks after injection of $5x10^6$ TC71-Luc cells. Treatment was started on day 0 followed by twice-weekly injections of the treatment formulations. (A) = 5% glucose, (B) = Naked siEFBP2, (C) = Tf-targeted nanoparticles containing siCON1, (D) = Tf-targeted nanoparticles containing siEFBP2, (E) = Non-targeted nanoparticles containing siEFBP2.

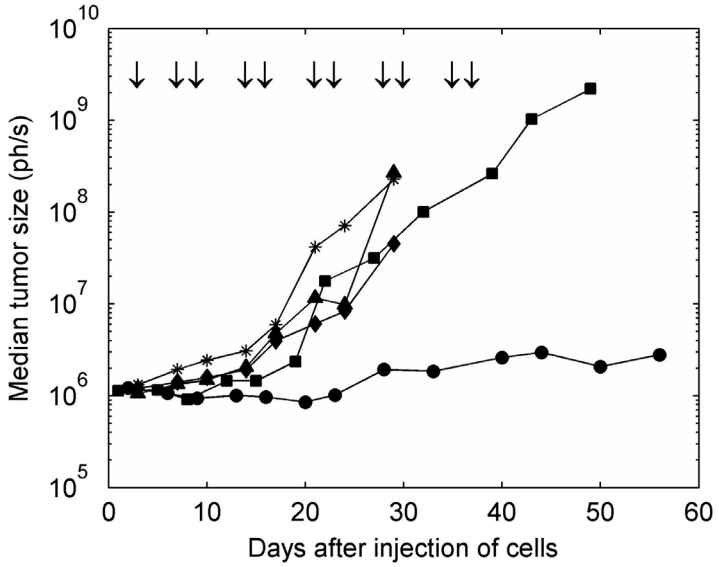

Figure 6.4. Median tumor size in NOD/scid mice after injection of $5x10^6$ TC71-Luc cells on day 0 followed by twice-weekly injections (arrows) of the treatment formulations. Circles = Tf-targeted nanoparticles containing siEFBP2, squares = non-targeted nanoparticles containing siEFBP2, diamonds = Tf-targeted nanoparticles containing siCON1, triangles = naked siEFBP2, and asterisks = 5% glucose.

6.4.4 No immune response or major organ damage was observed after treatment with targeted nanoparticles

Since the ability of the NOD/scid mice to mount a possible immune response to these formulations is severely compromised, single tail-vein injections of formulations were repeated in immunocompetent mice (C57BL/6) and blood was collected at 2 h or 24 h after the injections. Complete blood counts (CBC) of whole blood showed insignificant changes in white blood cell (WBC) or platelet (PLT) counts (Figure 6.5). Levels of secreted liver enzymes (AST, ALT), blood urea nitrogen (BUN), and creatinine (CRE) were all unchanged, indicating a lack of damage to the liver or kidneys. No increases, resulting from formulations, in plasma interleukin-12 (IL-12) or interferon-alpha (IFN-α) at either 2 h or 24 h post-injection were observed (Figure 6.5).

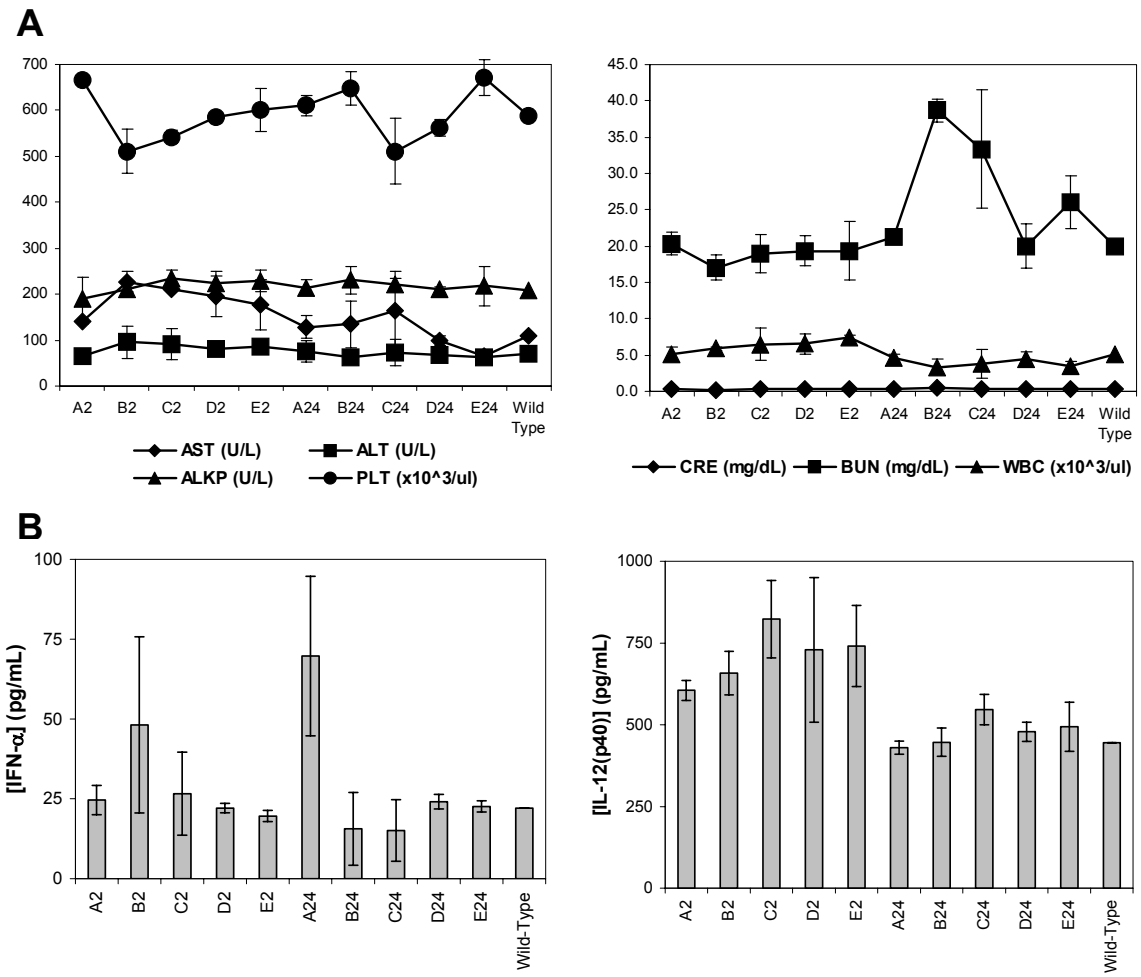

Figure 6.5. Evaluation of toxicity and immune response in mice after a single intravenous administration of formulated siRNA. (A) CBC and liver panel results for female C57BL/6 mice after a single intravenous dose of formulated siRNA. At 2 h or 24 h post-treatment, blood was drawn by cardiac puncture and plasma was isolated. Whole blood was used for determination of platelet (PLT) and white blood cell (WBC) counts. Plasma was used for measurement of aspartate aminotransferase (AST), alanine aminotransferase (ALT), alkaline phosphatase (ALKP), creatinine (CRE), and blood urea nitrogen (BUN). The averages of triplicate mice for each time point are plotted; error bars represent standard deviations. (B) Cytokine ELISA results for C57BL/6 mice after a single intravenous dose of formulated siRNA. The plasma levels of interleukin-12 (IL-12 (p40)) and interferon-alpha (IFN-α) in mice described above were measured by ELISA. Treatment groups: A = 5% glucose, B = naked siEFBP2, C = Tf-targeted nanoparticles containing siCON1, D = Tf-targeted nanoparticles containing siEFBP2, E = non-targeted nanoparticles containing siEFBP2, Wild-type = untreated. 2 = blood drawn 2 h after injection, 24 = blood drawn 24 h after injection.

We also performed pathological examination of the major organs (liver, kidney, brain, heart, lung, and pancreas) from the NOD/scid mice that received long-term treatments by hematoxylin and eosin (H&E) staining (Figure 6.6). No organ damage was observed with the nanoparticle formulations when compared to the 5% glucose and naked siEFBP2 treatment groups. Taken together, these results demonstrate the safety and low immunogenicity of these CDP-based nanoparticles.

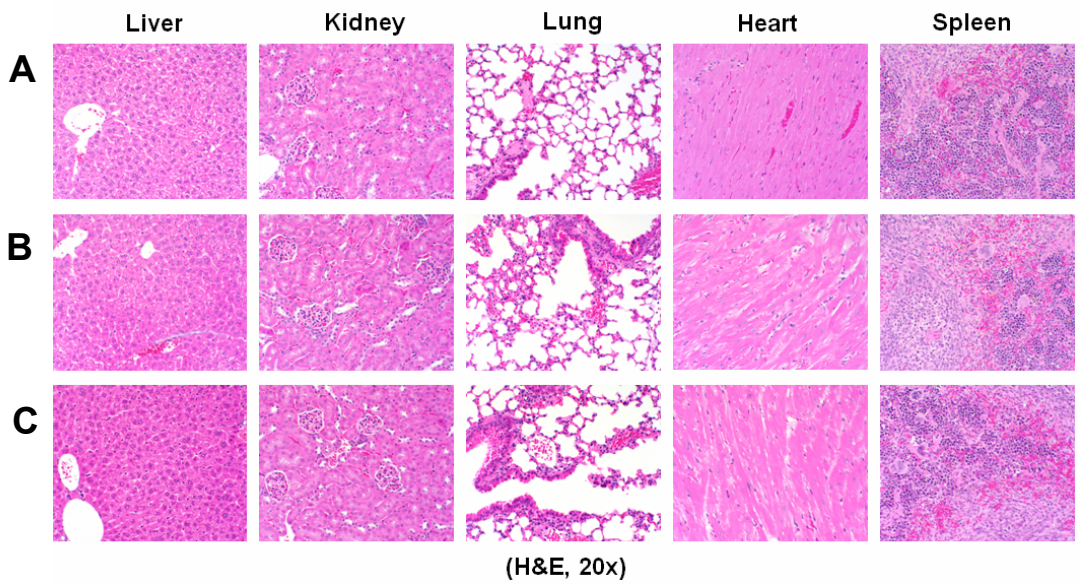

Figure 6.6. H&E staining of tissues from mice receiving long-term treatment with (A) 5% glucose, (B) naked siEFBP2, and (C) Tf-targeted nanoparticles containing siCON1.

6.5 Discussion

In this study, we describe the establishment of a highly reproducible and clinically relevant metastatic murine model for the Ewing's family of tumors in NOD/scid mice. Additionally, transduction of the EFT cells with the firefly luciferase gene enabled noninvasive, in vivo imaging of the mice to follow the fate of the injected tumor cells.

The tumor engraftment sites observed (lung, vertebral column, pelvis, femur and soft tissue) were comparable to the most common locations of metastases in EFT patients.

Small interfering RNA (siRNA) duplexes targeting the EWS-FLI1 fusion gene (siEFBP2) were formulated with CDP as described in Chapter 4. Targeted nanoparticles contained the transferrin targeting ligand to interact with the high levels of surface transferrin receptors expressed on the TC71 cells. This delivery system self-assembles with siRNA to form nanoparticles that are 60-80 nm in diameter.

Clinically, many tumors relapse after intensive treatment because of systemic dissemination of micrometastases. Nearly all EFT patients already have micrometastases at diagnosis, resulting in a >95% relapse rate when treated locally (2), and a 40% relapse rate after systemic chemotherapy (3). Therefore, effective treatment for elimination of circulating or dormant metastasized tumor cells after traditional therapy is needed. We explored the possibility of using targeted siRNA nanoparticles for this purpose by administration of the nanoparticles twice-weekly beginning the same day as injection of TC71-Luc cells. Of the different formulations tests, only the targeted nanoparticles containing siEFBP2 were able to achieve long-term tumor growth inhibition (Figure 6.4). Neither naked siEFBP2 nor targeted nanoparticles containing a control siRNA sequence showed any effect on tumor growth inhibition relative to the control group receiving only the 5% glucose carrier fluid. These results demonstrate the necessity of the delivery vehicle for systemic application and the sequence-specificity of the observed inhibition. We hypothesize that treatment with the targeted formulation of siEFBP2 assists in the prevention of the initial establishment of tumors in these mice from the injected cells and

slows the growth of any tumors that develop by downregulating the expression of the oncogenic fusion protein EWS-FLI1.

Notably, mice treated with non-targeted nanoparticles containing siEFBP2 showed an initial delay in tumor growth. However, the growth rate of tumors that eventually developed were unaffected by continuation of this treatment. The enhanced permeability and retention effect (EPR) leads to the accumulation of macromolecules in solid tumors, and both targeted and non-targeted nanoparticles may be able to accumulate in the tumors by this mechanism (12). This tumor accumulation of non-targeted nanoparticles was also observed by PET imaging, as discussed in Chapter 5. While some small fraction of the non-targeted nanoparticles may have entered tumor cells after accumulation in the tumor microenvironment, the inclusion of the Tf targeting ligand likely increases the overall uptake of the nanoparticles through receptor-mediated endocytosis. This increased uptake is likely responsible for the enhanced efficacy of Tf-targeted nanoparticles relative to non-targeted nanoparticles.

Recent in vitro reports have shown that siRNA sequences and their method of delivery may trigger an interferon response (13,14). Additionally, in vivo delivery of siRNA by lipids has resulted in potent interferon responses (15-17). Here, single tail-vein injections of all of the formulations were performed in immunocompetent (C57BL/6) mice to enable measurement of numerous blood markers that are indicative of an immune response. In contrast to results obtained from the injection of poly (I:C), a known immunostimulator through interactions with Toll-like receptor 3 (TLR3) (18), none of the formulations showed any significant effects on the levels of IL-12, IFN-α, white blood cells, platelets, secreted liver enzymes (ALT and AST), BUN, or CRE (Figure 6.5). All

of these observations with formulated siRNA are consistent with previous work showing a lack of immune response to naked siRNA (18). The cyclodextrin-based delivery system does not produce an interferon response even when siRNA is used that contains a motif known to be immunostimulatory when delivered in vivo with lipids (16) (published sequence is within siCON1). These results show the safety and low immunogenicity of CDP-containing formulations and demonstrate the attractiveness of this methodology for systemic, targeted delivery of nucleic acids. The in vivo gene silencing effect of siRNA by our delivery system is transient, permitting fine-tuning of the intensity and interval of the treatment. For example, the frequency of administration can be tuned for use in combination with other agents, and the treatment can be terminated within a few days if necessary.

This study demonstrates that, in contrast to naked siRNA delivery, the targeted siRNA nanoparticles used here are efficacious at low siRNA doses and do not require chemical modification for efficacy in vivo. Furthermore, the modular design of this delivery system enables it to be modified for targeting other tumor types by switching the specific targeting ligand attached to the surface of the nanoparticles. Importantly, the siRNA nanoparticles do not elicit a detectable immune response and are well-tolerated at the doses required for efficacy. We believe this treatment has the potential to be developed into a useful method for inhibition of metastatic EFT growth and may also have broad applicability in cancer therapy.

6.6 Acknowledgments

The authors would like to thank Greg Jensen (Insert Therapeutics, Inc.) for measurement of cellular TfR levels and Hu Wong (CHLA Clinical Laboratory) for CBC and liver panel analyses. We thank Dr. Donald B. Kohn and Denise Petersen (CHLA Vector Core) for transduction of the TC71 cells and Dr. Hiroyuki Shimada and Minerva Mongeotti (CHLA Experimental Pathology Core) for processing of mouse autopsy tissues. S.H-L. was supported by an endowment in Molecular Genetics and Molecular Pathology from Las Madrinas at CHLA. J.D.H. acknowledges the Whitaker Foundation for a doctoral fellowship. D.W.B. acknowledges the National Science Foundation for a graduate research fellowship.

6.7 References

1. Ginsberg, J.P., Woo, S.Y., Johnson, M.E., Hicks, M.J. and Horowitz, M.E. (2002) In Pizzo, P. A. and Poplack, D. G. (eds.), *Principles and Practice of Pediatric Oncology*. Lippincott Williams & Wilkins, Philadelphia, pp. 973-1016.
2. Dahlin, D.C., Coventry, M.B. and Scanlon, P.W. (1961) Ewing's sarcoma. A critical analysis of 165 cases. *Am J Orthop*, **43-A,** 185-192.
3. Rodriguez-Galindo, C., Spunt, S.L. and Pappo, A.S. (2003) Treatment of Ewing sarcoma family of tumors: current status and outlook for the future. *Med Pediatr Oncol*, **40,** 276-287.
4. Tanaka, K., Iwakuma, T., Harimaya, K., Sato, H. and Iwamoto, Y. (1997) EWS-Fli1 antisense oligodeoxynucleotide inhibits proliferation of human Ewing's sarcoma and primitive neuroectodermal tumor cells. *J Clin Invest*, **99,** 239-247.
5. Maksimenko, A., Malvy, C., Lambert, G., Bertrand, J.R., Fattal, E., Maccario, J. and Couvreur, P. (2003) Oligonucleotides targeted against a junction oncogene are made efficient by nanotechnologies. *Pharm Res*, **20,** 1565-1567.
6. Maksimenko, A., Lambert, G., Bertrand, J.R., Fattal, E., Couvreur, P. and Malvy, C. (2003) Therapeutic potentialities of EWS-Fli-1 mRNA-targeted vectorized antisense oligonucleotides. *Ann N Y Acad Sci*, **1002,** 72-77.
7. Dohjima, T., Lee, N.S., Li, H., Ohno, T. and Rossi, J.J. (2003) Small interfering RNAs expressed from a Pol III promoter suppress the EWS/Fli-1 transcript in an Ewing sarcoma cell line. *Mol Ther*, **7,** 811-816.
8. Kovar, H., Ban, J. and Pospisilova, S. (2003) Potentials for RNAi in sarcoma research and therapy: Ewing's sarcoma as a model. *Semin Cancer Biol*, **13,** 275-281.
9. Chansky, H.A., Barahmand-Pour, F., Mei, Q., Kahn-Farooqi, W., Zielinska-Kwiatkowska, A., Blackburn, M., Chansky, K., Conrad, E.U., 3rd, Bruckner, J.D., Greenlee, T.K. et al. (2004) Targeting of EWS/FLI-1 by RNA interference attenuates the tumor phenotype of Ewing's sarcoma cells in vitro. *J Orthop Res*, **22,** 910-917.
10. Vormoor, J., Baersch, G., Decker, S., Hotfilder, M., Schafer, K.L., Pelken, L., Rube, C., Van Valen, F., Jurgens, H. and Dockhorn-Dworniczak, B. (2001) Establishment of an in vivo model for pediatric Ewing tumors by transplantation into NOD/scid mice. *Pediatr Res*, **49,** 332-341.
11. Zhang, J., Hu, S., Schofield, D.E., Sorensen, P.H. and Triche, T.J. (2004) Selective usage of D-Type cyclins by Ewing's tumors and rhabdomyosarcomas. *Cancer Res*, **64,** 6026-6034.
12. Tanaka, T., Shiramoto, S., Miyashita, M., Fujishima, Y. and Kaneo, Y. (2004) Tumor targeting based on the effect of enhanced permeability and retention (EPR) and the mechanism of receptor-mediated endocytosis (RME). *Int J Pharm*, **277,** 39-61.
13. Bridge, A.J., Pebernard, S., Ducraux, A., Nicoulaz, A.L. and Iggo, R. (2003) Induction of an interferon response by RNAi vectors in mammalian cells. *Nat Genet*, **34,** 263-264.

14. Sledz, C.A., Holko, M., de Veer, M.J., Silverman, R.H. and Williams, B.R. (2003) Activation of the interferon system by short-interfering RNAs. *Nat Cell Biol*, **5,** 834-839.
15. Hornung, V., Guenthner-Biller, M., Bourquin, C., Ablasser, A., Schlee, M., Uematsu, S., Noronha, A., Manoharan, M., Akira, S., de Fougerolles, A. et al. (2005) Sequence-specific potent induction of IFN-alpha by short interfering RNA in plasmacytoid dendritic cells through TLR7. *Nat Med*, **11,** 263-270.
16. Judge, A.D., Sood, V., Shaw, J.R., Fang, D., McClintock, K. and Maclachlan, I. (2005) Sequence-dependent stimulation of the mammalian innate immune response by synthetic siRNA. *Nat Biotechnol*, **23,** 457-462.
17. Ma, Z., Li, J., He, F., Wilson, A., Pitt, B. and Li, S. (2005) Cationic lipids enhance siRNA-mediated interferon response in mice. *Biochem Biophys Res Commun*, **330,** 755-759.
18. Heidel, J.D., Hu, S., Liu, X.F., Triche, T.J. and Davis, M.E. (2004) Lack of interferon response in animals to naked siRNAs. *Nat Biotechnol*, **22,** 1579-1582.
19. Davis, M.E., Pun, S.H., Bellocq, N.C., Reineke, T.M., Popielarski, S.R., Mishra, S. and Heidel, J.D. (2004) Self-assembling nucleic acid delivery vehicles via linear, water-soluble, cyclodextrin-containing polymers. *Curr Med Chem*, **11,** 179-197.